

CT patterns of organizing pneumonia in patients treated with VEGF/mTOR inhibitors for metastatic renal cell cancer: an observational study

Sabine Dettmer¹, Viktor Grünwald², Thomas Fuehner³, Arnold Ganser², Frank Wacker¹, Philipp Ivanyi^{2,*} and Thomas Rodt^{1,*}

Abstract

Background: Targeted therapies are the standard treatment in patients with metastatic renal cell carcinoma (mRCC) and are known to cause adverse pulmonary events. Organizing pneumonia (OP) with its various manifestations in computed tomography (CT) has therefore lately received more attention.

Purpose: To describe the spectrum of CT patterns of OP in patients with mRCC receiving targeted therapies.

Material and Methods: Seventeen patients with known therapy-related OP were analyzed retrospectively by two blinded radiologists in consensus. Images were scored according to OP patterns that have previously been described. Additionally, the distribution and the predominant imaging pattern in each patient were determined.

Results: In our cohort, ground glass opacity was the most common imaging pattern (17/17, 100%) in patients with OP followed by a reticular pattern (12/17, 71%), consolidations (10/17, 59%), nodules (7/17, 41%), crazy paving (5/17, 29%), bronchi(ol)ectasis (4/17, 24%), focal mass (3/17, 18%), and reversed halo (1/17, 6%). The most common imaging pattern was changing multifocal consolidations (8/17, 47%). A bronchocentric and a nodular pattern were found in four patients (24%) each, a progressive fibrotic pattern in none patient, and reversed halo/atoll pattern in one (6%) case.

Conclusion: OP is the major differential diagnosis to be considered in patients with targeted therapies and pulmonary changes. Knowledge of the variety of imaging findings can facilitate diagnosis.

Keywords

Organizing pneumonia, interstitial lung disease, computed tomography (CT), targeted therapy, renal cell cancer

Date received: 2 October 2016; accepted: 24 January 2017

Introduction

Organizing pneumonia (OP) is a non-specific pathologic pattern of the lung in response to injury and can occur idiopathic and secondary. Common causes of secondary OP are drugs, infections, immunologic disorders, and inhalation of toxic substances (1,2). Although OP has been well-known since the early 1970s, it has recently moved more into the focus of interest due to the new era of targeted therapies. Histologically it is often characterized by intra-alveolar buds of granulation tissue (2,3). The clinical presentation is unspecific and with varying degrees of clinical severity ranging from no symptoms to cough, fever, malaise, fatigue, and weight

¹Department of Diagnostic and Interventional Radiology, Hannover Medical School, Hannover, Germany

²Department of Haematology, Haemostasis, Oncology and Stem Cell Transplantation, Hannover Medical School, Hannover, Germany

³Department of Respiratory Medicine, Hannover Medical School, Hannover, Germany

*Equal contributors.

Corresponding author:

Sabine Dettmer, Department of Diagnostic and Interventional Radiology, Hannover Medical School, Carl-Neuberg-Str. 1, 30625 Hannover, Germany.

Email: Dettmer.sabine@mh-hannover.de



loss, or even death (3,4). The main features of OP on chest computed tomography (CT) are airspace consolidations and ground glass opacities (GGO), typically with either a bilateral subpleural and basal or a peribronchial distribution. Other manifestations of OP include nodular and reticular patterns (5). Clinical observation paired with radiological observations mostly allows an appropriate diagnosis of an OP.

Targeted therapies are currently the standard treatment in patients with metastatic renal cell carcinoma (mRCC) (6). This type of treatment uses new drugs that selectively attack specific types of cancer cells blocking special biological and cytological features involved in the growth and spread of cancer cells. The two main modes of action of targeted agents aim dominantly either at the vascular-endothelial-growth-factor receptor (VEGFR), or the mammalian-target-of-rapamycin (mTOR) signaling pathways. Sunitinib is a VEGFR inhibitor which mainly blocks angiogenesis (6). Temozolomide and everolimus inhibit mTOR signaling causing changes of cellular metabolism, transcription, translation, proliferation, and angiogenesis (7). Targeted therapy implies chronic drug exposure and often causes unusual adverse effects like OP; this has been described for patients treated with VEGFR inhibitors (8–10) but particularly in patients receiving mTOR inhibitors (8,11–13).

The aim of this retrospective study was to analyze CT imaging features of OP in mRCC patients receiving targeted therapies at our tertiary care center.

Material and Methods

Study design

This single-center study was approved by the internal review board of Hannover Medical School (no. 1820-2013). Patients' electronic medical charts were retrospectively analyzed. Patient data were anonymized and analyses were performed in concordance with the Declaration of Helsinki in its latest revised version.

Patients with mRCC treated with sunitinib, everolimus, or temsirolimus from January 2006 until December 2009 at Hannover Medical School were included as described before in a retrospective clinical analysis not addressing the CT morphological findings (8). Patients with OP were followed until August 2012. The patients received everolimus (10 mg once a day), temsirolimus (25 mg i.v. weekly), or sunitinib (50 mg 4-2 schedule orally) after informed consent. Dosing and dose reductions were conducted according to the summary of product characteristics. CT was performed according to local standards for routine tumor assessment every two to three months or when clinically indicated.

Clinical diagnosis of OP

Diagnosis of OP was made by the treating physician (medical oncologist) in consensus with a pulmonologist. The diagnosis of OP was primarily based on presenting symptoms (e.g. cough, dyspnea, fever) and the clinical course. Further diagnostics, including serological, microbiological, and virological tests, ECG, pulmonary function tests, bronchoscopy, and CT, were performed according to institutional standards. Bronchoalveolar lavage and transbronchial biopsy were performed if clinically indicated. For the diagnosis of a drug-induced interstitial lung disease, no other reason than the therapy at risk had to be apparent as the underlying cause, as previously described (8).

CT data acquisition and scoring

CT examinations were performed for evaluation of a variety of clinical presentations in the internal radiology department or externally. Internal CT examinations were carried out with a 64-row MDCT (Lightspeed VCT, GE Healthcare, Milwaukee, WI, USA) or a 16-row MDCT (Lightspeed 16, GE Healthcare); intravenous contrast medium was used if necessary for proper assessment of the clinical indication. CT data were acquired using 120 kV, 100 mAs, a rotation time of 0.8 s, and a pitch of 0.984, the slice collimation during acquisition was 1.25. Axial 1.25 mm slices with an interval of 1 mm were reconstructed. The field of view (FOV) was adapted to the size of the patient's lung. External CT examinations were performed with varying protocols. Only CT examinations performed in a time period \pm 30 days from the date of organizing pneumonia diagnosis were included.

Retrospective evaluation of CT images was performed in all patients with clinically diagnosed OP. Consensus reading and scoring was carried out by two chest radiologists (SD and TR), both with five years of experience in thoracic CT. Pathological findings other than pulmonary metastases were evaluated. Images were scored for abnormalities associated with drug-induced lung changes previously described in the literature (e.g. consolidations, GGO, nodules, reversed halo) on a scale from 0 (not present) to 2 (clearly present); 1 was used, if the pattern was minimally present and not dominant. Abnormalities were defined according to the Fleischner Society nomenclature (14). Additional features like micro and macro or sharp or unsharp for nodules and the anatomic distribution (subpleural, peribronchial, random) were also registered. Finally, the dominant imaging pattern was determined as "changing multifocal peripheral consolidations," "bronchocentric pattern," "solitary focal mass or nodule," "nodular pattern," "multiple masses or larger nodules," "progressive fibrotic

pattern,” “perilobular pattern,” “band like pattern,” “reversed halo/atoll pattern,” or “crazy paving” according to Robertson et al. (5).

Results

Characteristics of patients with OP during treatment with targeted agents

During the observation period, 125 mRCC patients were identified who received 205 courses of chemotherapy (134 courses of sunitinib, 55 courses of everolimus, and 16 courses of temsirolimus). Thereof, 20 cases of OP were identified, reflecting an overall OP incidence of 10%. OP was most common with the mTOR inhibitor everolimus ($n=14/55$, 25%), while no OP was identified in patients treated with temsirolimus. Furthermore, OP was also identified in patients treated with the VEGF inhibitor sunitinib with a frequency of 3% ($n=6/205$). Median time between treatment initiation and onset of OP was 3.6 months.

Of these 20 patients, CT examinations at the time of OP diagnosis \pm 30 days were available in 18 patients; one patient had to be excluded because of a severe infection of the lung. Descriptive data of the 17 patients analyzed in this study are given in Table 1.

The median age of the patients was 54 years (age range, 32–84; 9 men, 8 women). All patients suffered from mRCC; the time from primary diagnosis to metastasis was 18.2 months (range, 0–156.6 months). Four patients had been treated with sunitinib (VEGFR inhibitor) and 13 with everolimus (mTOR inhibitor). Bronchoalveolar lavage was available in 11/17 (65%) and transbronchial biopsies in 7/17 (41%) patients. These could exclude infectious disease and lymphangiosis as differential diagnosis and results were consistent with OP.

Radiological findings in mRCC patients with OP due to targeted therapies

The median time between diagnosis of OP and CT examination was 0 days (range, 0–24 days).

Consolidations (Figs. 1 and 2) were present in ten patients (59%), six of these (60%) showed an air bronchogram (Table 2, Fig. 1). All patients showed GGO. Nodules were present in seven patients (41%), four with predominantly macronodules and three with micronodules, three with sharp margins and four with unsharp margins. A focal mass was seen in three patients (18%) and a reversed halo pattern in one patient (6%) (Fig. 3). A reticular pattern was present in 12 patients (71%), five (29%) displayed crazy paving, none showed honeycombing. Four patients (24%) had traction bronchiectasis or

Table 1. Descriptive data for patients with OP in our study cohort.

Parameter	Number/median
Patients with OP (%)	20/125 (16)
OP patients included in analyses (n)	17/20
Median age at diagnosis of RCC (years (range))	54 (32–84)
Median age at initiation of treatment associated with OP (years (range))	62 (44–85)
Gender (n (%))	
Male	9 (53)
Female	8 (47)
Histology of RCC	
Clear cell	17 (100%)
MSKCC score	
Low	4
Intermediate	6
High	0
Not evaluated	7
Median time from RCC diagnosis to metastasis, median (months (range))	18.2 (0–156.6)
Therapy at onset of organizing pneumonia (n (%))	
sunitinib (VEGFR inhibitor)	4/17 (24)
everolimus (mTOR inhibitor)	13/17 (76)
Median time between treatment initiation and onset of OP (months (range))	3.6 (2.1–21.5)

MSKCC, Memorial Sloan-Kettering Cancer Center Score for Metastatic Renal Cell Carcinoma.

bronchiolectasis and 11 (65%) presented with an architectural distortion (Table 2). OP patients with sunitinib had consolidations more often than those with everolimus (100% versus 46%); nodules were less frequent in patients with sunitinib (25% versus 46%). All other imaging features showed a similar frequency (Table 2). Nevertheless, the number of patients was too small for further statistical group comparisons.

The predominant pattern (Table 3) was characterized as changing multifocal peripheral consolidations in eight patients (47%, Fig. 1). In four patients (24%) it was a bronchocentric pattern (Fig. 2) and in a further four patients (24%) a nodular pattern. No patient showed a progressive fibrotic pattern and one patient had a reversed halo pattern (6%, Fig. 3).

The anatomical distribution of the different patterns was random in most cases. The bronchocentric pattern and the nodular pattern were mainly located peribronchially. A subpleural distribution was seen in patients with changing multifocal peripheral consolidations or a progressive fibrotic pattern.

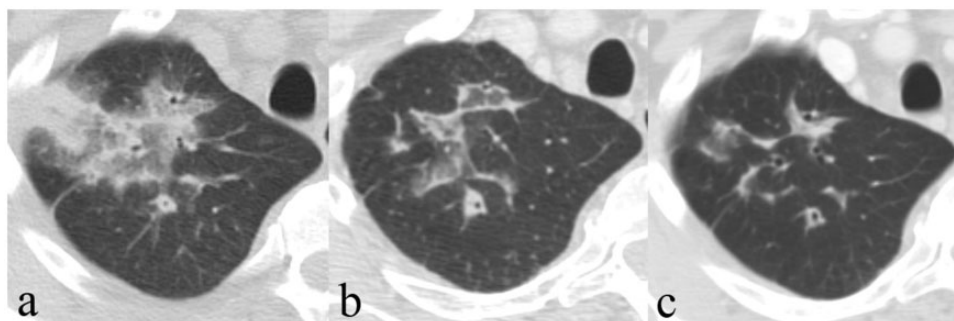


Fig. 1. CT of a 56-year-old male patient with changing multifocal consolidation typical of OP at the time point of diagnosis (a). The patient received the mTOR inhibitor everolimus for treatment of metastatic renal cell cancer. Typical are the adjacent ground glass opacities and the air bronchogram. The follow-up studies three weeks (b) and ten weeks later (c) show an incomplete resolution of the consolidation in the right upper lobe.

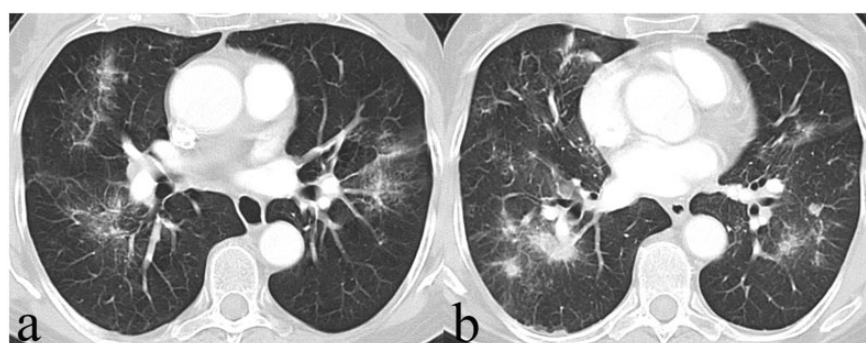


Fig. 2. A 49-year-old woman with a bronchocentric pattern of OP due to targeted therapy with sunitinib (VEGFR inhibitor). CT shows multiple bilateral consolidations located along the bronchovascular bundles, some with surrounding ground glass opacities.

Table 2. CT pattern in patients with OP during targeted therapy and their frequency in all patients with OP and separately for those with sunitinib and everolimus treatment.

Pattern in CT	All patients (n = 17)	Sunitinib (n = 4)	Everolimus (n = 13)
Consolidation	10 (59%)	4 (100%)	6 (46%)
Ground glass opacities	17 (100%)	4 (100%)	13 (100%)
Nodules	7 (41%)	1 (25%)	6 (46%)
Focal mass	3 (18%)	1 (25%)	2 (15%)
Radial bands	0 (0%)	0 (0%)	0 (0%)
Reversed halo	1 (6%)	0 (0%)	1 (8%)
Crazy paving	5 (29%)	1 (25%)	4 (31%)
Reticular pattern	12 (71%)	3 (75%)	9 (69%)
Architectural distortion	11 (65%)	3 (75%)	8 (62%)
Honeycombing	0 (0%)	0 (0%)	0 (0%)
Tration bronchi(ol)ectasis	3 (%)	0 (0%)	3 (23%)

Discussion

The aim of the current study was to analyze CT imaging patterns of OP in mRCC patients receiving

targeted therapy and to describe the variety of patterns in CT. The most predominant features in our cohort were GGO which were present in each patient. Consolidations were also common and were detected in 59% of patients. Consolidations and GGO have already been described to be the most common patterns in OP (15). Regarding various publications of the last two decades summarized in Table 4 (16–28), consolidations were described in about 70–100% and GGO in about 60–100% of cases (Table 4) (16,19,21). Thus, in our cohort consolidations were within the lower end of previously published data (Table 4).

The distribution of findings has been described to be predominantly peripheral and subpleural, referred to as multifocal peripheral consolidations, or around the bronchovascular structures, referred to as bronchocentric pattern (5). In our study population, changing multifocal peripheral consolidations were the predominant imaging pattern (47%, Fig. 1); this is in agreement with previously published data (5). The consolidations are typically changing in location over time. The distribution is usually described as peripheral and basal but there was also a study, which found an equal craniocaudal distribution (28) which is in accordance with our results. The consolidations in our patient group mainly

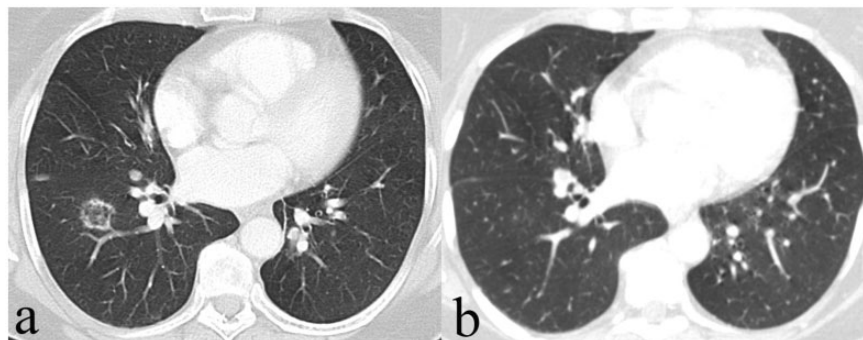


Fig. 3. Reversed halo pattern (also referred to as atoll-sign) in a 50-year-old woman who received everolimus for treatment of renal cell cancer. CT shows a classic reversed halo pattern with focal area of GGO surrounded by a ring of consolidation (a). The finding resolved within four months as shown by the follow-up CT (b).

Table 3. Predominant pattern in patients with OP during targeted therapy, their frequency and predominant anatomical distribution in all patients with OP and separately for those with sunitinib and everolimus treatment.

Predominant pattern	All patients (n = 17)	Distribution	Sunitinib (n = 4)	Everolimus (n = 13)
Changing multifocal peripheral consolidations	8 (47%)	Random 4 Subpleural 2	2 (50%)	6 (46%)
Bronchocentric	4 (24%)	Peribronchial 3 Random 1	2 (50%)	2 (15%)
Progressive fibrotic pattern	0		0	0
Nodular pattern	4 (24%)	Peribronchial 3 Subpleural 1	0 (0%)	4 (31%)
Reversed halo/Atoll pattern	1 (6%)	Random 1	0 (0%)	1 (8%)

contained air bronchograms (60%) and some were associated with areas of GGO which has previously been described (3,28,29).

The bronchocentric pattern is characterized by consolidations forming conspicuous cuffs around larger bronchovascular bundles (5). We found this pattern to be predominant in four patients (24%) (Fig. 2). This is in accordance with Robertson et al., who reported the bronchocentric pattern to be observed in up to one-third of patients (5). Lower lobe predominance was described in a part of the patients. Co-existence with subpleural consolidations, GGO, and a nodular pattern has been reported (25).

We found nodules in 41% and a predominant nodular pattern in 24% of cases. In previous studies, nodules were reported to be frequent in patients with OP and occurred in about 15–70% (Table 4); a predominant nodular pattern has been described in up to 30% of patients (21). Morphology is heterogeneous and a distinction for size (micronodular ≤ 4 mm, macronodular), and margins (sharp, unsharp) can be made. The differentiation to nodules of other cause might be difficult

especially in patients with pulmonary metastases and bronchiolitis. In this situation, the clinical presentation and the appearance of the nodules may help; e.g. an ill-defined micronodular pattern with centrilobular distribution more likely resembles an exudative bronchiolitis and is a less common manifestation of OP (29). The most common appearance in patients with OP is lesions with an irregular or spiculated margin (30).

The progressive fibrotic pattern shows basal reticulation and architectural distortion. It typically co-exists with, or follows, regions of consolidation or GGO (5). In the literature, this pattern was less frequent compared to changing multifocal peripheral consolidations and the bronchocentric pattern and occurred in up to one-quarter of patients (28). In our study, the progressive fibrotic pattern was predominant in none patient. The time point of CT might be crucial for the diagnosis since the progressive fibrosis probably develops over time and occurs as predominant pattern at a later stage which we did not evaluate in our study.

The atoll or reversed halo pattern is rare, but has been regularly described in patients with OP. Originally

Table 4. Frequency of the patterns consolidations, ground glass opacities (GGO), and nodules in patients with OP found in CT. Results of this study and a survey of the literature with the number of patients (n) and the percentage of findings are displayed.

Study	n	Consolidations (%)	GGO (%)	Nodules (%)
This study	17	59	100	41
Arakawa, 2001 (16)	38	87	58	32
Greenberg-Wolff, 2005 (17)	8	100	50	75
Jara-Palomares, 2010 (18)	21	43	10	10
Johkoh, 1999 (19)	24	83	100	63
Kim, 2003 (20)	31	87	90	42
Lee, 1994 (21)	43	79	60	30
Lee, 2003 (22)	26	62	88	NE
Lee, 2010 (23)	22	77	86	32
Mehrian, 2014 (24)	31	71	84	36
Müller, 1990 (25)	14	71	NE	50
Okada, 2009 (26)	37	81	65	14
Preidler, 1996 (27)	15	100	33	13
Ujita, 2004 (28)	21	95	86	24

NE, not evaluated.

the reversed halo pattern was regarded as relatively specific for OP, but since its first description it has also been described in numerous other conditions including granulomatosis with polyangiitis and infectious disease (31,32). We found the reversed halo sign in a single patient with OP (6%) (Fig. 3).

Further patterns like a solitary focal mass or nodule, multiple masses or larger nodules, a perilobular pattern, the band like pattern or crazy paving have been less frequently described in patients with OP and were not observed in our study group.

The major limitation of our study is the small number of patients (n=17) reflecting a single center experience, and possibly a selection bias due to the retrospective analysis and the limitation on patients receiving a CT in clinical routine. However, OP is not very frequent and not always evaluated by CT. Most studies on this topic are based on a limited number of cases. Our results may therefore contribute to an overall assessment of radiological pattern in OP.

To determine the predominant pattern can be difficult, especially without longitudinal analysis and if there is co-existence of different imaging features. Furthermore, pre-existing pulmonary changes like metastases, lymphangiosis, or pneumonia make it difficult or even impossible to determine OP-related lung changes, if there is no previous imaging analysis. This

and the high variability of appearance in CT may contribute to the varying published data for imaging patterns of OP. Thus, our study contributes to the further characterization of imaging features in patients with OP in the specific context of targeted therapies.

In conclusion, CT imaging features of OP in patients with targeted therapy show a high variability even though GGO and consolidations are seen in the majority of cases in our cohort. OP is the major differential diagnosis to be considered in patients with targeted therapy and pulmonary changes. Knowledge of the variability of imaging findings presented in this paper can facilitate diagnosis.

Declaration of conflicting interests

The author(s) declared no potential conflicts of interest with respect to the research, authorship, and/or publication of this article.

Funding

The author(s) received no financial support for the research, authorship, and/or publication of this article.

References

1. Einollahi B, Aslani J, Taghipour M, et al. Sirolimus-induced bronchiolitis obliterans organizing pneumonia in a kidney transplant recipient; a case report and review of literature. *J Nephropathol* 2014;3:109–113.
2. Sulavik SB. The concept of “organizing pneumonia”. *Chest* 1989;96:967–969.
3. Cordier JF. Cryptogenic organising pneumonia. *Eur Respir J* 2006;28:422–446.
4. Epler GR, Colby TV, McLoud TC, et al. Bronchiolitis obliterans organizing pneumonia. *N Engl J Med* 1985; 312:152–158.
5. Robertson BJ, Hansell DM. Organizing pneumonia: a kalidoscope of concepts and morphologies. *Eur Radiol* 2011;21:2244–2254.
6. Escudier B, Eisen T, Porta C, et al. ESMO Guidelines Working Group. Renal cell carcinoma: ESMO Clinical Practice Guidelines for diagnosis, treatment and follow-up. *Ann Oncol* 2012;23(Suppl 7): vii65–vii71.
7. Hidalgo M, Rowinsky EK. The rapamycin-sensitive signal transduction pathway as a target for cancer therapy. *Oncogene* 2000;19:6680–6686.
8. Ivanyi P, Fuehner T, Adam M, et al. Interstitial lung disease during targeted therapy in metastatic renal cell carcinoma: a case series from three centres. *Med Oncol* 2014;131:147.
9. Morelon E, Stern M, Israel-Biet D, et al. Characteristics of sirolimus-associated interstitial pneumonitis in renal transplant patients. *Transplantation* 2001;72:787–790.
10. Weiner SM, Sellin L, Vonend O, et al. Pneumonitis associated with sirolimus: clinical characteristics, risk factors and outcome—a single-centre experience and review of the literature. *Nephrol Dial Transplant* 2007;22:3631–3637.

11. Dabydeen DA, Jagannathan JP, Ramaiya N, et al. Pneumonitis associated with mTOR inhibitors therapy in patients with metastatic renal cell carcinoma: incidence, radiographic findings and correlation with clinical outcome. *Eur J Cancer* 2012;48:1519–1524.
12. Baas MC, Struijk GH, Moes DJ, et al. Interstitial pneumonitis caused by everolimus: a case-cohort study in renal transplant recipients. *Transpl Int* 2014;27:428–436.
13. Champion L, Stern M, Israel-Biet D, et al. Brief communication: sirolimus-associated pneumonitis: 24 cases in renal transplant recipients. *Ann Intern Med* 2006;144:505–509.
14. Hansell DM, Bankier AA, MacMahon H, et al. Fleischner Society: glossary of terms for thoracic imaging. *Radiology* 2008;246:697–722.
15. Travis WD, Costabel U, Hansell DM, et al. ATS/ERS Committee on Idiopathic Interstitial Pneumonias. An official American Thoracic Society/European Respiratory Society statement: Update of the international multidisciplinary classification of the idiopathic interstitial pneumonias. *Am J Respir Crit Care Med* 2013;188:733–748.
16. Arakawa H, Kurihara Y, Niimi H, et al. Bronchiolitis obliterans with organizing pneumonia versus chronic eosinophilic pneumonia: high-resolution CT findings in 81 patients. *Am J Roentgenol* 2001;176:1053–1058.
17. Greenberg-Wolff I, Konen E, Ben Dov I, et al. Cryptogenic organizing pneumonia: variety of radiologic findings. *Isr Med Assoc J* 2005;7:568–570.
18. Jara-Palomares L, Gomez-Izquierdo L, Gonzalez-Vergara D, et al. Utility of high-resolution computed tomography and BAL in cryptogenic organizing pneumonia. *Respir Med* 2010;104:1706–1711.
19. Johkoh T, Müller NL, Cartier Y, et al. Idiopathic interstitial pneumonias: diagnostic accuracy of thin-section CT in 129 patients. *Radiology* 1999;211:555–560.
20. Kim SJ, Lee KS, Ryu YH, et al. Reversed halo sign on high-resolution CT of cryptogenic organizing pneumonia: diagnostic implications. *Am J Roentgenol* 2003;180:1251–1254.
21. Lee KS, Kullnig P, Hartman TE, et al. Cryptogenic organizing pneumonia: CT findings in 43 patients. *Am J Roentgenol* 1994;162:543–546.
22. Lee JS, Lynch DA, Sharma S, et al. Organizing pneumonia: prognostic implication of high-resolution computed tomography features. *J Comput Assist Tomogr* 2003;27:260–265.
23. Lee JW, Lee KS, Lee HY, et al. Cryptogenic organizing pneumonia: serial high-resolution CT findings in 22 patients. *Am J Roentgenol* 2010;195:916–922.
24. Mehrian P, Shahnazi M, Dahaj AA, et al. The spectrum of presentations of cryptogenic organizing pneumonia in high resolution computed tomography. *Pol J Radiol* 2014;79:456–460.
25. Müller NL, Staples CA, Miller RR. Bronchiolitis obliterans organizing pneumonia: CT features in 14 patients. *Am J Roentgenol* 1990;154:983–987.
26. Okada F, Ando Y, Honda K, et al. Comparison of pulmonary CT findings and serum KL-6 levels in patients with cryptogenic organizing pneumonia. *Br J Radiol* 2009;82:212–218.
27. Preidler KW, Szolar DM, Moelleken S, et al. Distribution pattern of computed tomography findings in patients with bronchiolitis obliterans organizing pneumonia. *Invest Radiol* 1996;31:251–255.
28. Ujita M, Renzoni EA, Veeraraghavan S, et al. Organizing pneumonia: peribular pattern at thin-section CT. *Radiology* 2004;232:757–761.
29. Müller NL, Miller R. Diseases of the bronchioles: CT and histopathologic findings. *Radiology* 1995;196:3–12.
30. Akira M, Yamamoto S, Sakatani M. Bronchiolitis obliterans organizing pneumonia manifesting as multiple large nodules or masses. *Am J Roentgenol* 1998;170:291–295.
31. Agarwal R, Aggarwal AN, Gupta D. Another cause of reverse halo sign: Wegener's granulomatosis. *Br J Radiol* 2007;80:849–850.
32. Gasparetto EL, Escuissato DL, Davaus T, et al. Reversed halo sign in pulmonary paracoccidioidomycosis. *Am J Roentgenol* 2005;184:1932–1934.